

# Computational Investigation of the Effect of Chemistry on Mars Retropropulsion Environments using a Massively Parallel GPU Approach

Gabriel Nastac<sup>1</sup>, Aaron Walden<sup>1</sup>, Eric Nielsen<sup>1</sup>, Ashley Korzun<sup>1</sup>, Christopher Stone<sup>2</sup>, Patrick Moran<sup>3</sup>















<sup>1</sup>NASA Langley Research Center

<sup>2</sup>National Institute of Aerospace

<sup>3</sup>NASA Ames Research Center

# Introduction

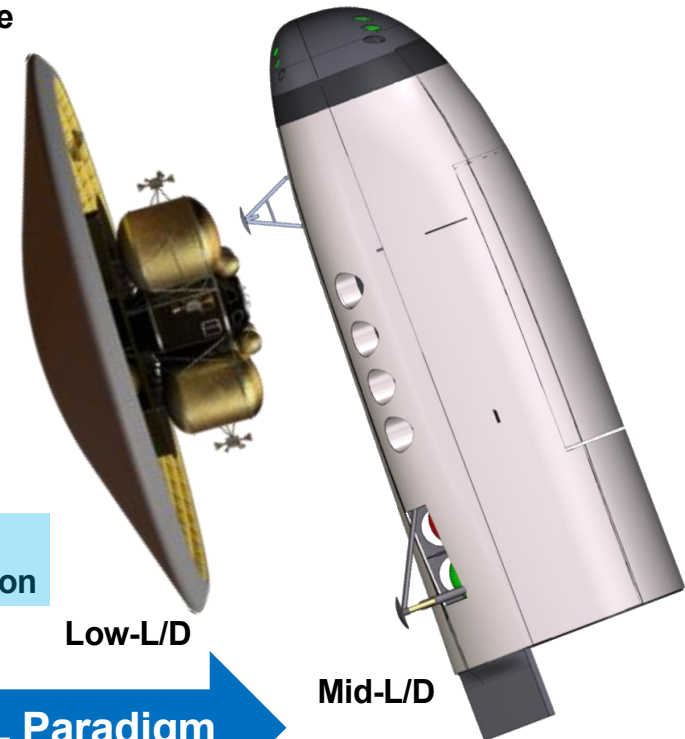
- Heritage Entry, Descent, and Landing (EDL) systems cannot land masses required for human Mars exploration
- Supersonic parachutes cannot be extended to high-mass EDL
- Propulsive descent and landing are enabling for human-scale EDL at Mars
- Legacy ground test data (1960s – early 1970s) and modern NASA investments form the current basis of experience

	Viking	Pathfinder	MER	Phoenix	MSL	InSight	M2020
Entry Capsule							
Diameter (m)	3.505	2.65	2.65	2.65	4.52	2.65	4.5
Entry Mass (t)	0.930	0.584	0.832	0.573	3.153	0.608	3.440
Parachute Diameter (m)	16.0	12.5	14.0	11.8	19.7	11.8	21.5
Parachute Deploy (Mach)	1.1	1.57	1.77	1.65	2.2	1.66	1.75
Landed Mass (t)	0.603	0.360	0.539	0.364	1.75	0.375	1.050
Landing Altitude (km)	-3.5	-2.5	-1.4	-4.1	-4.4	-2.6	-2.5
Terminal Descent and Landing Technology	 Retro-propulsion	 Airbags	 Airbags	 Retro-propulsion	 Skycrane	 Retro-propulsion	 Skycrane

Human-Scale Lander (Projected)

16 - 19  
49 - 65  
N/A  
N/A  
26 - 36  
0

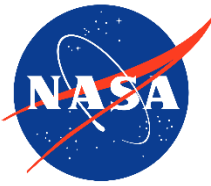
Supersonic Retropropulsion



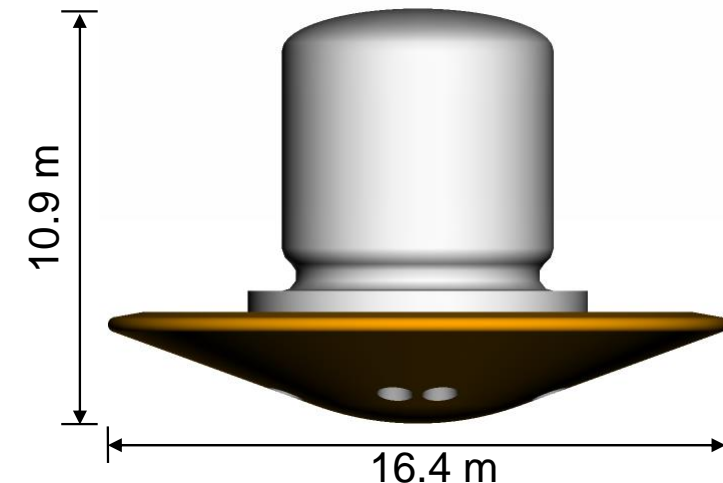
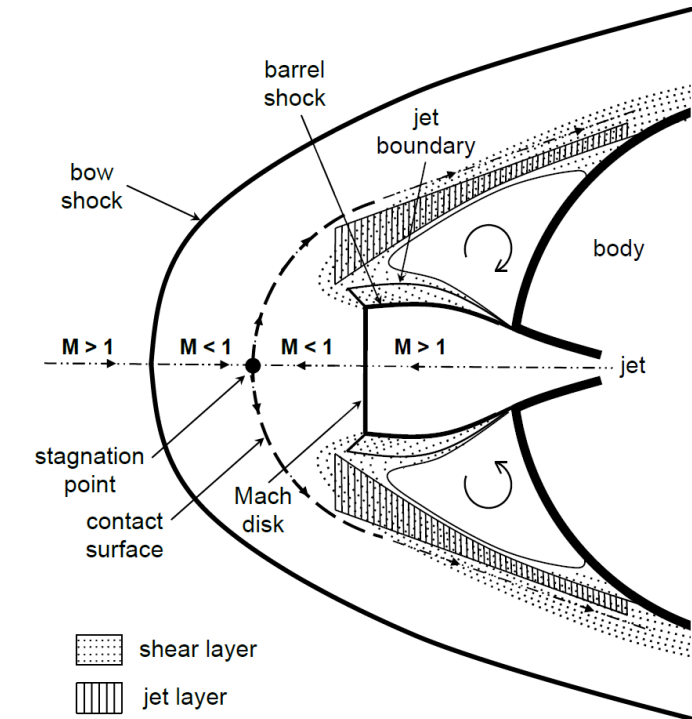
Steady progression of “in family” EDL

New EDL Paradigm

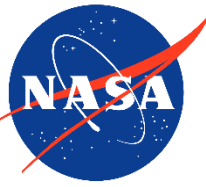
# Motivation



- **Vehicle design requires understanding aerodynamic-propulsive interference effects**
- Retropropulsion ground tests require significant compromises on physical scale, instrumentation, configuration, and environments
- Past simulation and experimental work primarily focused on perfect gas flows
- Past simulation work by the authors investigated a Mars lander concept scaled for perfect gas air
- Recently, chemically reacting CFD simulations of the Mars lander concept at realistic Martian conditions have been carried out on Summit
  - Simulations used up to ~16,000 V100s and simulated seconds of physical time for various conditions along a proposed descent trajectory



# Governing Equations and Numerical Implementation



- NASA FUN3D<sup>1</sup> is the flow solver used for this work
- Node-based finite-volume approach on general unstructured grids
- Thermochemical Nonequilibrium (“Generic Gas”) path is used
- Conservation of species, momentum, energies, and turbulence variables
- Two-temperature model available for thermal nonequilibrium
- 2 equation models (e.g., SST), Spalart-Allmaras turbulence model with Catris-Aupoix compressibility correction; DES option
- Variable species, energies, and turbulence equations
- Fully implicit formulations are used to integrate the equations in time
  - Sparse block linear system:  $A\mathbf{x} = \mathbf{b}$
  - Matrix  $A$  composed of diagonal and off-diagonal  $N_{eq} \times N_{eq}$  blocks
  - Memory and solution time increases as  $O(N_{eq}^2)$
- System solved with multicolor point-implicit approach

<sup>1</sup><https://fun3d.larc.nasa.gov/>

$$\begin{aligned}\frac{\partial}{\partial t}(\rho y_s) + \frac{\partial}{\partial x_j}(\rho y_s u_j) - \frac{\partial}{\partial x_j}(J_{sj}) &= \dot{\omega}_s \\ \frac{\partial}{\partial t}(\rho u_i) + \frac{\partial}{\partial x_j}(\rho u_i u_j + p \delta_{ij}) - \frac{\partial}{\partial x_j}(\tau_{ij}) &= 0 \\ \frac{\partial}{\partial t}(\rho E) + \frac{\partial}{\partial x_j}((\rho E + p)u_j) - \frac{\partial}{\partial x_j}\left(u_k \tau_{kj} + \dot{q}_j + \sum_{s=1}^{N_s} h_s J_{sj}\right) &= 0 \\ \frac{\partial}{\partial t}(\rho E_v) + \frac{\partial}{\partial x_j}(\rho E_v u_j) - \frac{\partial}{\partial x_j}\left(\dot{q}_{vj} + \sum_{s=1}^{N_s} h_{vs} J_{sj}\right) &= S_v \\ \frac{\partial}{\partial t}(\rho \tilde{v}) + \frac{\partial}{\partial x_j}(\rho \tilde{v} u_j) - \frac{\partial}{\partial x_j}\left(\frac{1}{\sigma} \left( \mu \frac{\partial \tilde{v}}{\partial x_j} + \sqrt{\rho} \tilde{v} \frac{\partial \sqrt{\rho} \tilde{v}}{\partial x_j} \right)\right) &= S_{\tilde{v}}\end{aligned}$$

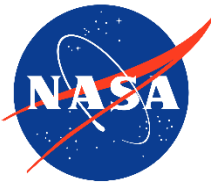
$$\mathbf{q} = [\rho \vec{y}_s, \rho \vec{u}, \rho E, \rho E_v, \rho \tilde{v}]^T$$

$$\int_V \frac{\partial \mathbf{q}}{\partial t} dV + \oint_S (\mathbf{F} \cdot \mathbf{n}) dS - \int_V \mathbf{S} dV = \mathbf{0}$$

$$\left[ \frac{V}{\Delta \tau} \mathbf{I} + \frac{V}{\Delta t} \mathbf{I} + \frac{\partial \hat{\mathbf{R}}}{\partial \mathbf{q}} \right] \Delta \mathbf{q} = -\mathbf{R}(\mathbf{q}^{n+1,m}) - \frac{V}{\Delta t} (\mathbf{q}^{n+1,m} - \mathbf{q}^n)$$

$$\mathbf{q}^{n+1,m} = \mathbf{q}^{n+1,m} + \Delta \mathbf{q}$$

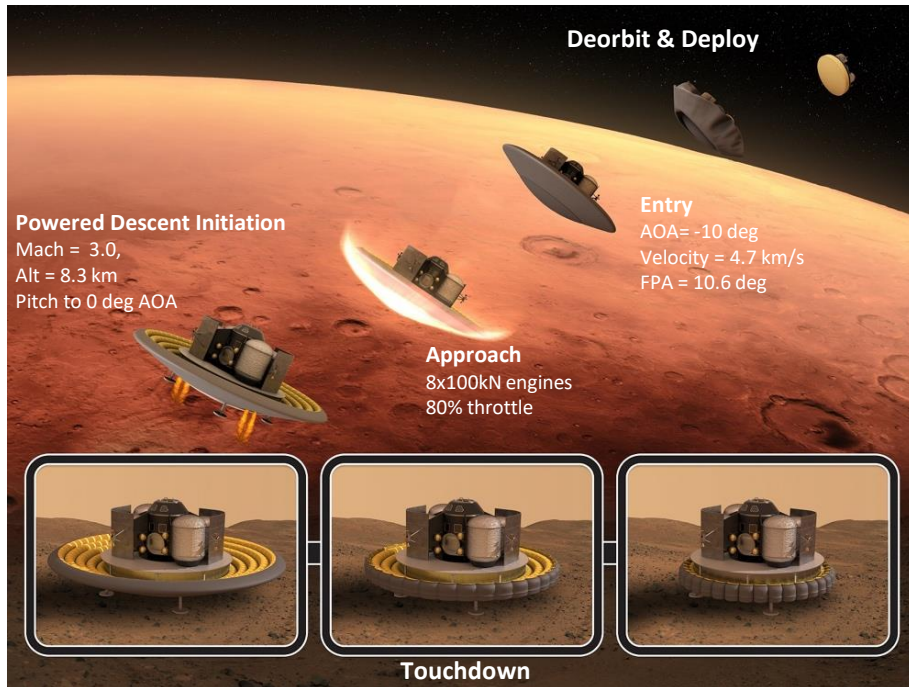
# FLUDA



- FLUDA is a CUDA-based C++ port of compute kernels in FUN3D
- Currently written using a thin layer above AMD Heterogeneous Interface for Portability (HIP) enabling:
  - NVIDIA GPUs (through native CUDA)
  - AMD GPUs (through HIP)
- Other frameworks/approaches are being considered in the frame of performance portability
  - We aim to reach a good percentage of peak memory bandwidth on key kernels such as linear algebra
- Many kernels employ hierarchical parallelism, especially for chemistry related kernels<sup>1</sup>
  - Many threads work on an item such as a flux or Jacobian
  - Threads/item and items/block are parameterized
  - Parameters are tuned by an automated process for each device and equation set, which may result in hundreds of different parameter settings for each kernel
  - Tuning has improved performance by over 5x for some kernels

<sup>1</sup>Gabriel Nastac, Aaron Walden, Eric J. Nielsen, and Kader Frendi, "Implicit Thermochemical Nonequilibrium Flow Simulations on Unstructured Grids using GPUs," AIAA 2021-0159, 2021.

# INCITE Efforts



Summit efforts include:

- Scale resolved perfect gas retropropulsion simulations to match limited experiments on Earth that use air as exhaust
- Scale resolved chemically reacting retropropulsion simulations to match a realistic vehicle
  - Methane combustion in Martian CO<sub>2</sub> atmosphere
  - ~10x more computationally expensive than perfect gas

## Campaign Goals

- **Science:** Advance the understanding of retropropulsion flow physics during Mars EDL of a human-scale lander
- **Computational:** Demonstrate production readiness and efficiency advantages of GPU implementation of the FUN3D CFD code at scale

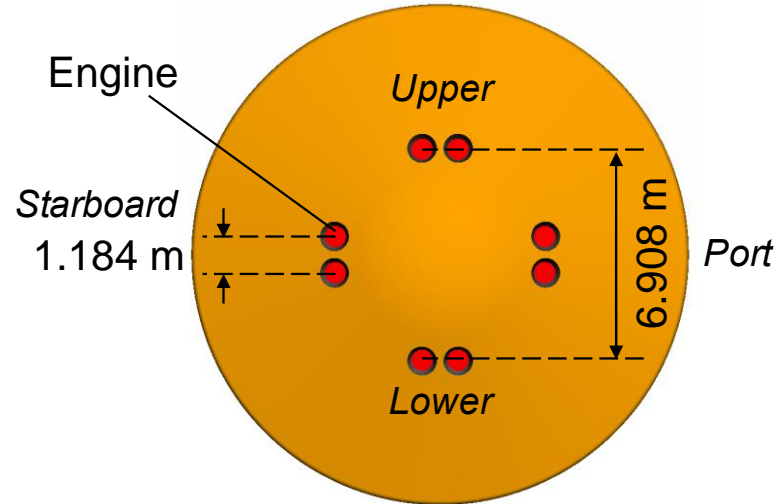
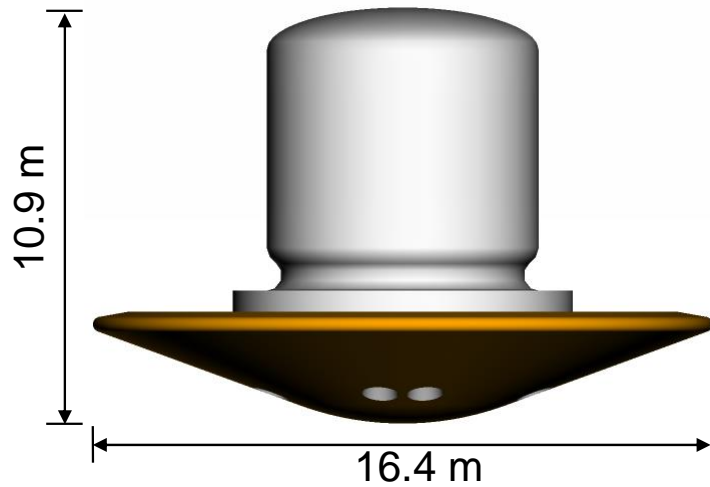
Ashley M. Korzun, Eric Nielsen, Aaron Walden, William Jones, Jan-Reneé Carlson, Patrick Moran, Christopher Henze and Timothy Sandstrom. "Computational Investigation of Retropropulsion Operating Environments with a Massively Parallel Detached Eddy Simulation Approach," AIAA 2020-4228. ASCEND 2020. November 2020.

Ashley M. Korzun, Gabriel Nastac, Aaron Walden, Eric J. Nielsen, William T. Jones and Patrick Moran. "Application of a Detached Eddy Simulation Approach with Finite-Rate Chemistry to Mars-Relevant Retropropulsion Operating Environments," AIAA 2022-2298. AIAA SCITECH 2022 Forum. January 2022.

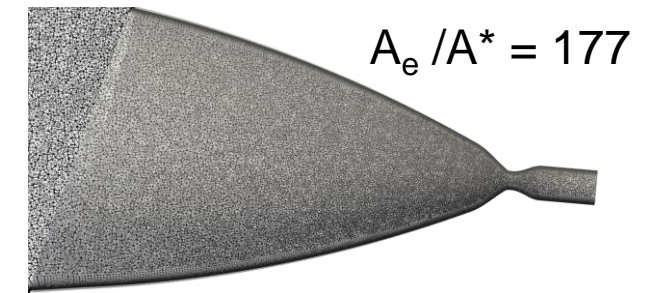
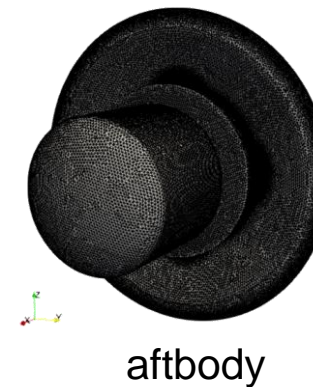
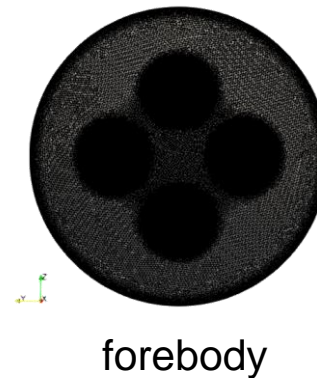
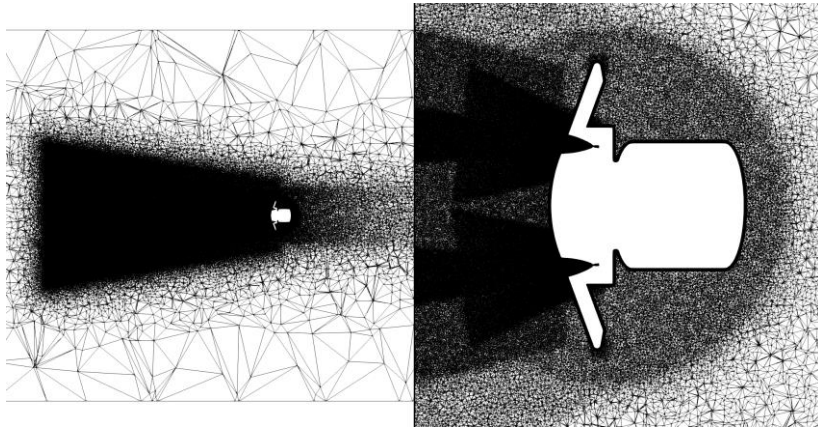
Gabriel Nastac, Ashley M. Korzun, Aaron Walden, Eric J. Nielsen, William T. Jones and Patrick Moran. "Computational Investigation of the Effect of Chemistry on Mars Supersonic Retropropulsion Environments," AIAA 2022-2299. AIAA SCITECH 2022 Forum. January 2022.



# Vehicle Model and Grid



- Full 3-D geometry
- Engines canted  $5^\circ$  and scarfed to a flush intersection
- Domain dimensions in *kilometers* with the ability to resolve flow features on the order of centimeters
- Approximately 1.1 billion grid points (subsonic grid is  $\sim 15\%$  larger)
- Walls resolved with  $y^+ \approx 1$



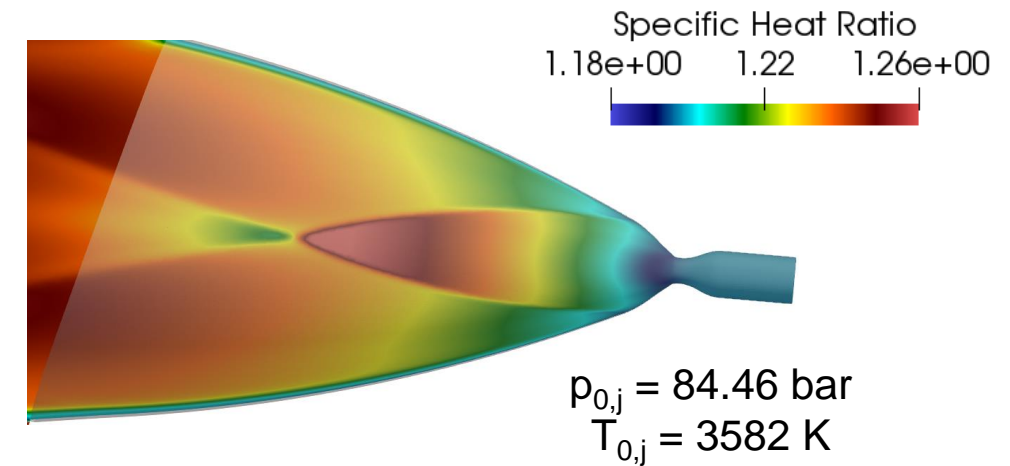
All grid images taken from initial 139 million point grid

# Conditions

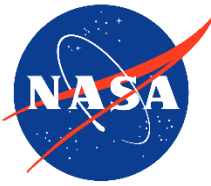
- Supersonic, transonic, and subsonic points along human-scale Mars powered descent trajectory
  - 80% throttle for all 8 engines
  - ~ 31 seconds required to decelerate from Mach 2.4 to 0.8
- Vehicle maintains shallow flight path angle and  $0^\circ$  angle of attack
- Mars atmosphere (97%  $\text{CO}_2$ , 3%  $\text{N}_2$ ) and  $\text{O}_2/\text{CH}_4$  combustion products ( $\text{O}/\text{F} = 3.5$ )
- 10-species, 19-reaction chemical mechanism
- Full nozzle is modeled, including the boundary layer and non-equilibrium effects

## Freestream Conditions

$M_\infty$	$V_\infty$ (m/s)	$T_\infty$ (K)	$p_\infty$ (Pa)	$q_\infty$ (Pa)	$\rho_\infty$ (kg/m <sup>3</sup> )
2.40	560.60	216.53	284.73	1,093.82	0.0070
1.40	329.37	218.63	386.48	507.85	0.0094
0.80	189.10	219.50	442.92	191.16	0.0107





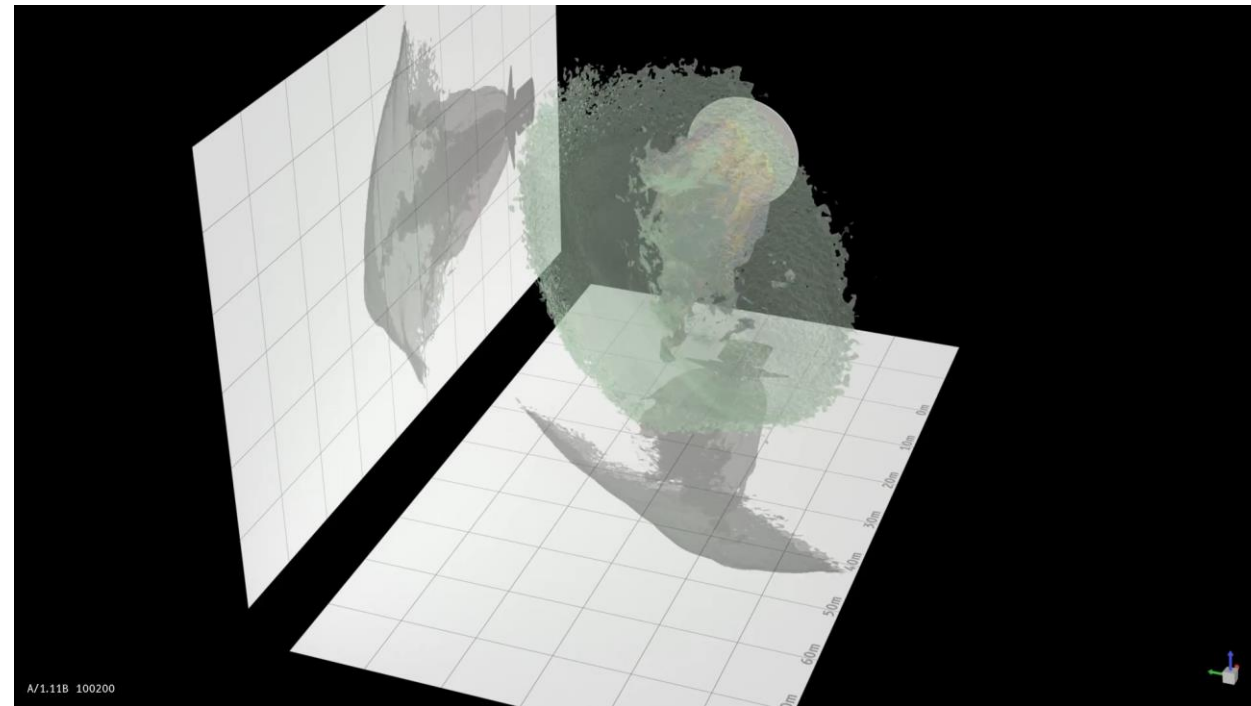
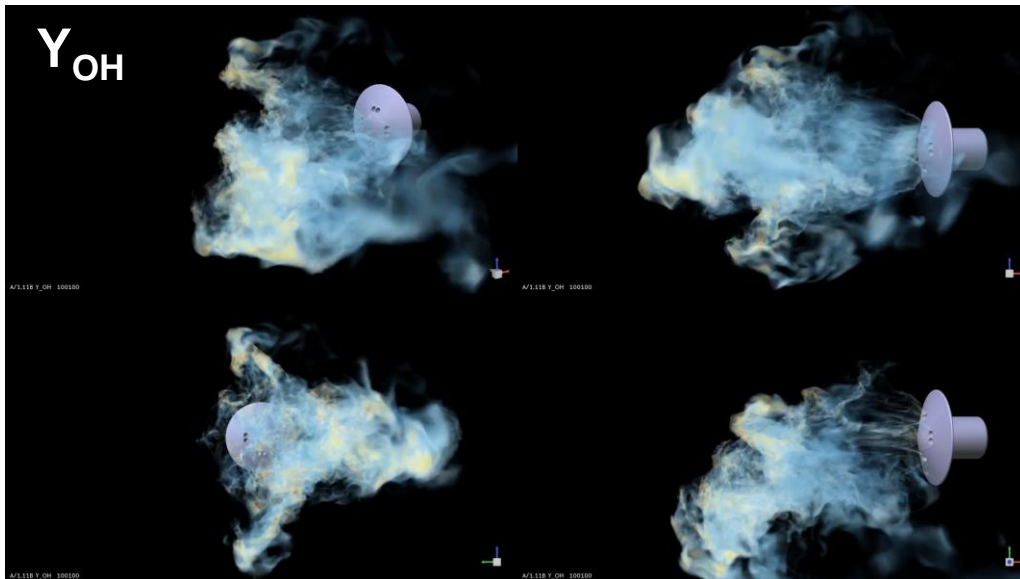
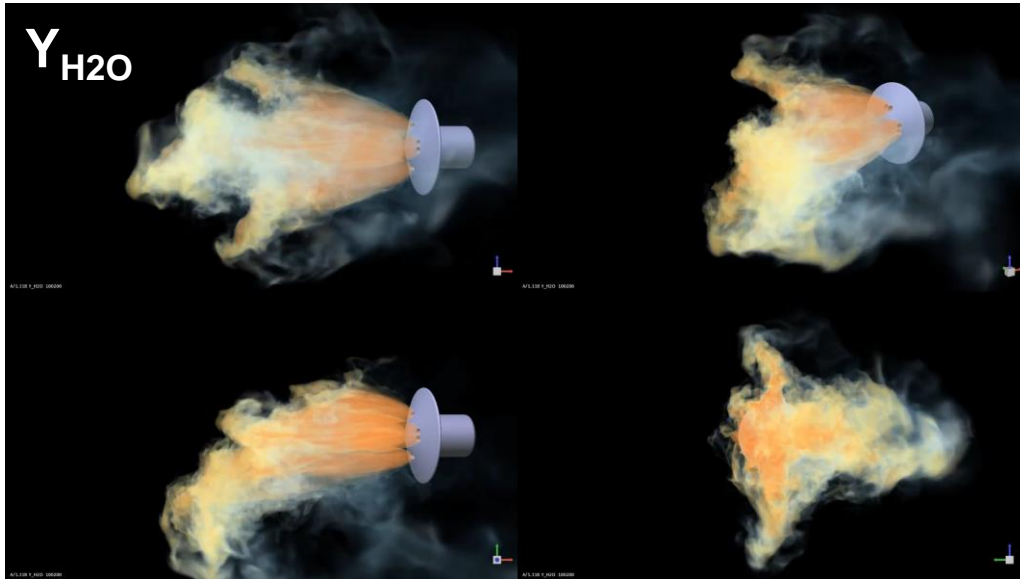


# Performance Overview

- 1 V100 ~ 400 x86 CPU cores for the physics and computational setup in this work
  - 15 PDEs, fully implicit ( $15^2$  Jacobians)
- Simulations are carried out using 20% to about 60% of the Summit machine
- Asynchronously saving variables (~100 GB) every 50 time steps for the entire simulation
  - Less than 1% runtime overhead
  - Roughly 600 TB data/run
- Global CFL  $O(100+)$ , due to the turbulent BL resolution requirements in the nozzle

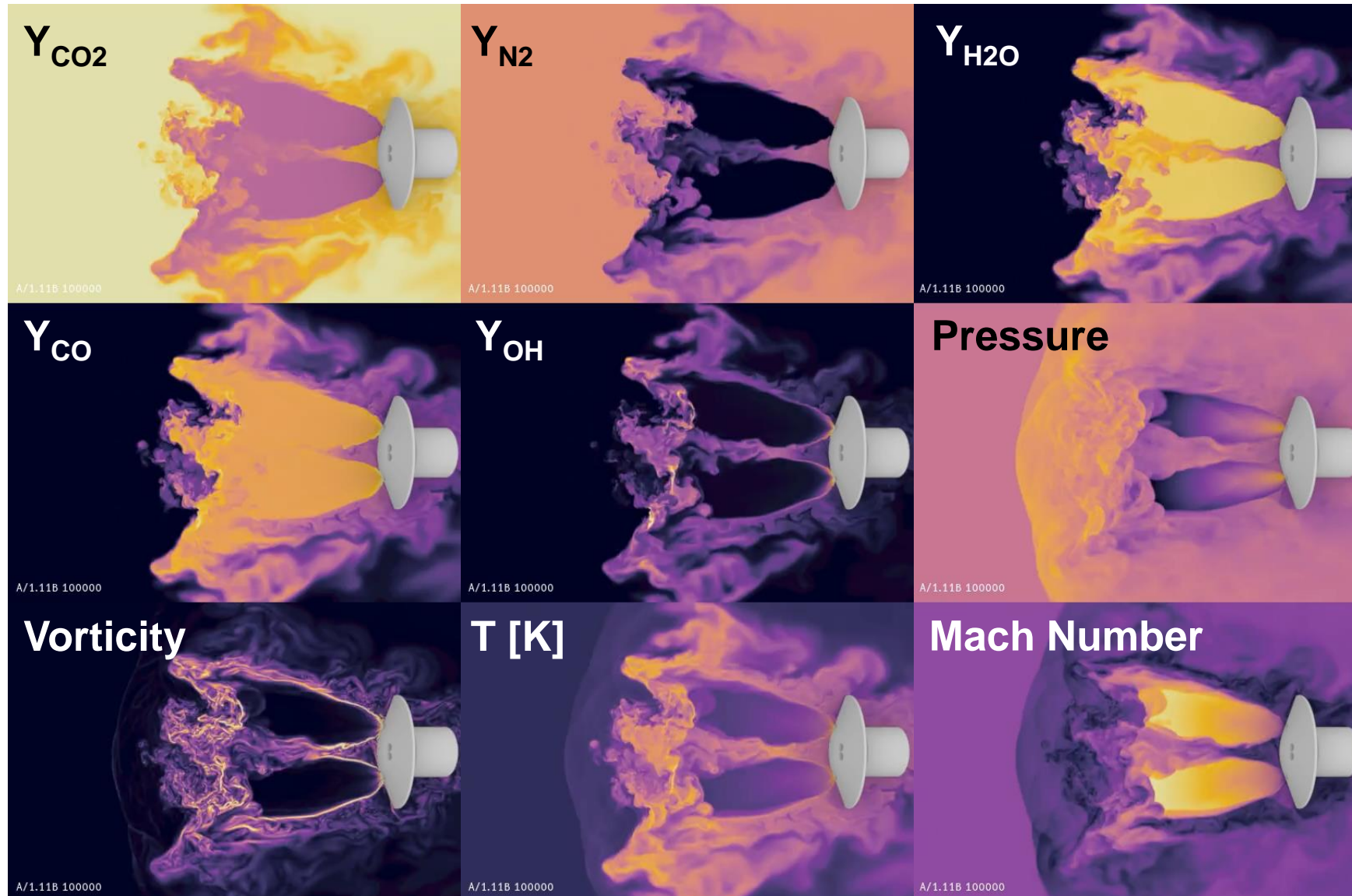
Case	Time Step [ $\mu$ s]	Global CFL	GPUs	Points / GPU	Wall Time [s] / Time Step
$M_\infty = 2.4$	8.6	225	5,532	200,000	1.18
$M_\infty = 1.4$	14.6	384	13,824	80,000	0.62
$M_\infty = 0.8$	25.4	668	15,912	80,000	0.61

# Flowfield Visualization for Mach 2.4 (1/3)

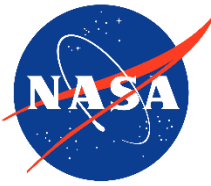


Isosurfaces of  $Y_{H_2O}$  (0.4) colored by vorticity magnitude and bow shock  
(each Cartesian grid line represents 10 meters)

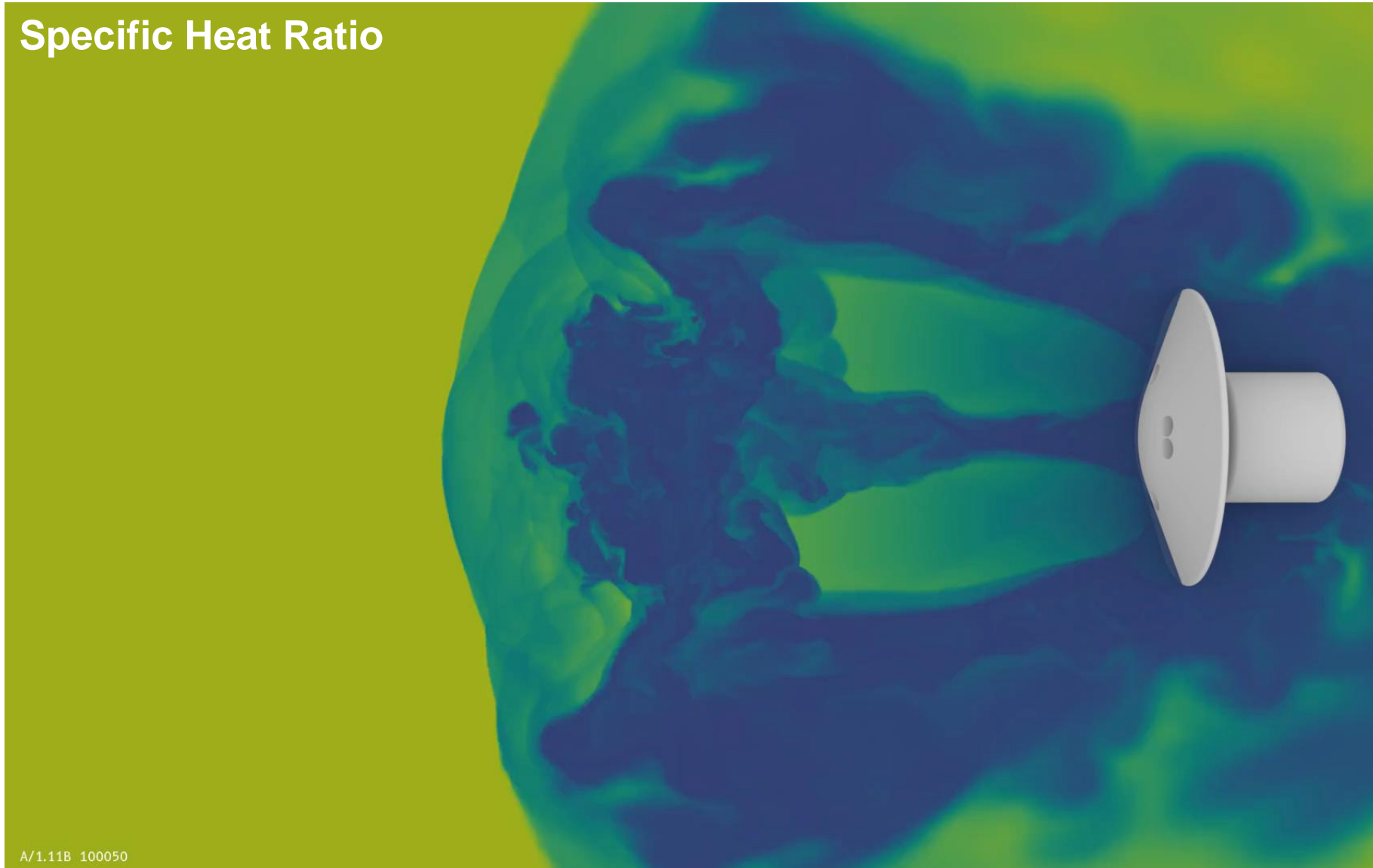
# Flowfield Visualization for Mach 2.4 (2/3)



# Flowfield Visualization for Mach 2.4 (3/3)

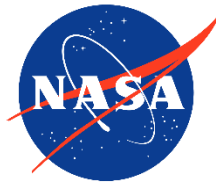


Specific Heat Ratio

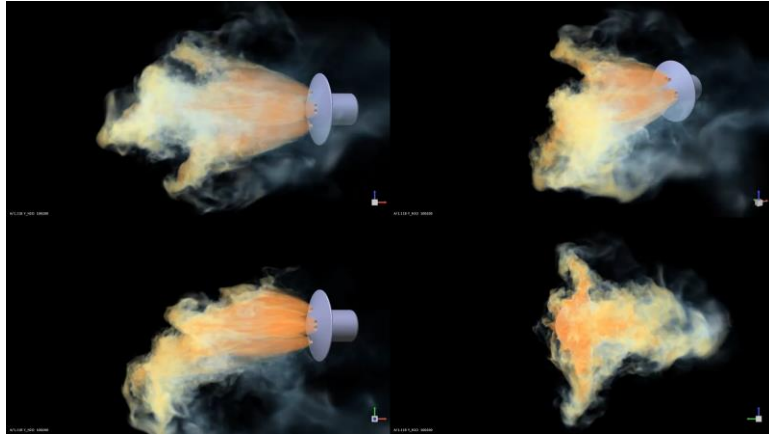




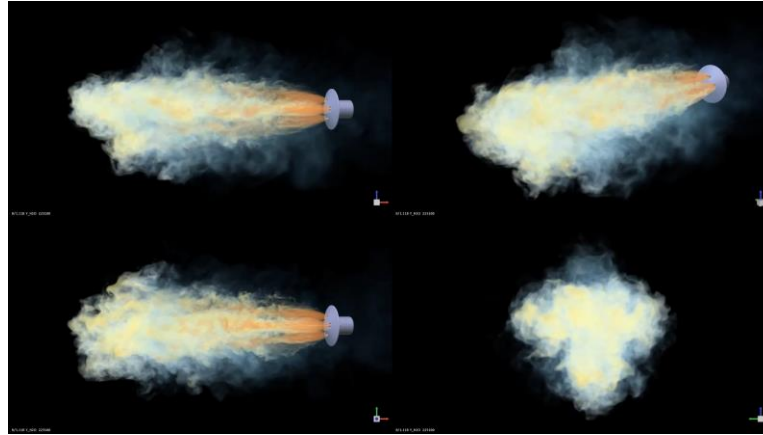
# Flowfield Visualization for All Conditions



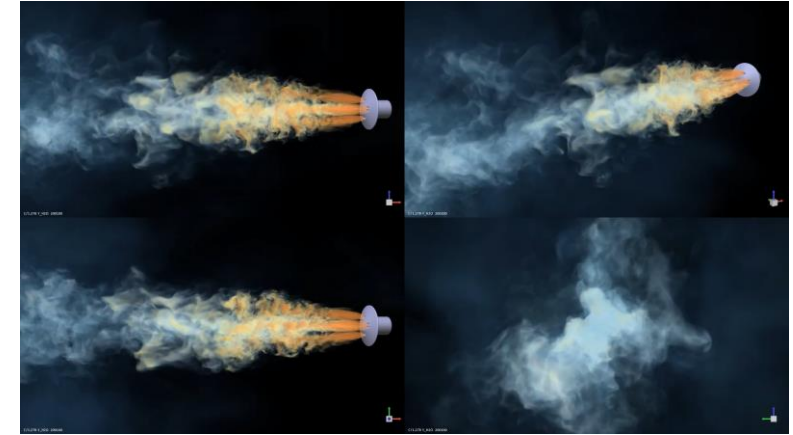
$M_\infty = 2.4$



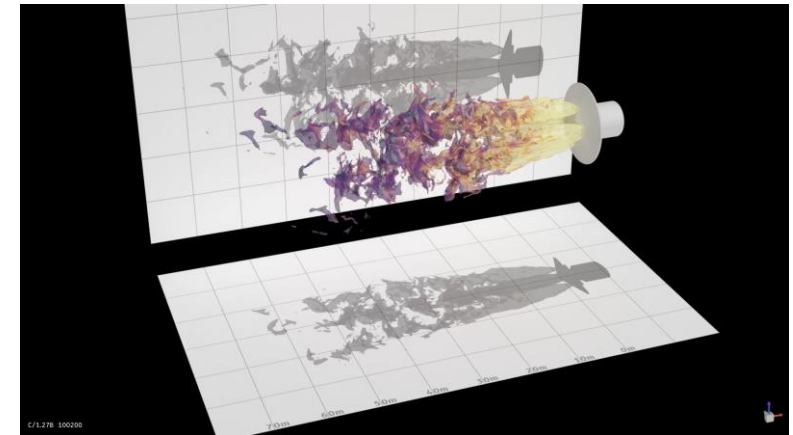
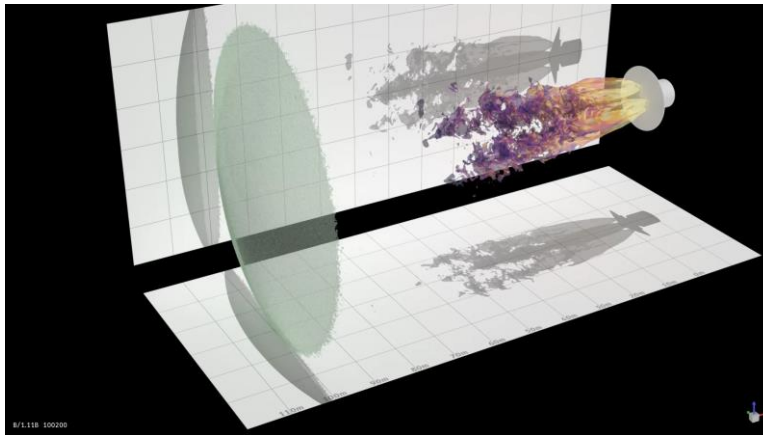
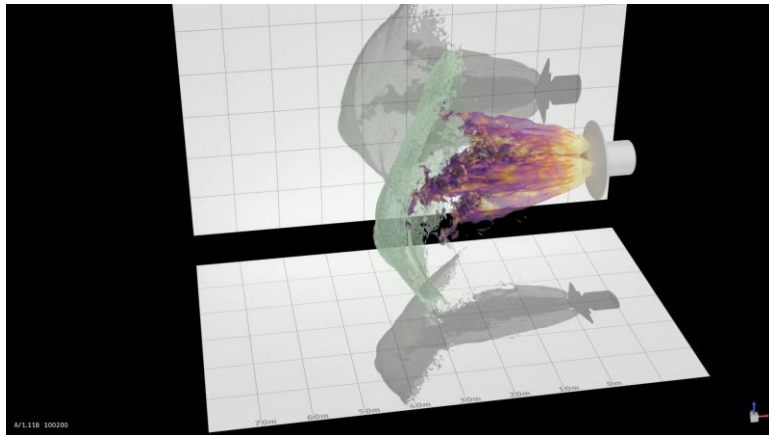
$M_\infty = 1.4$



$M_\infty = 0.8$

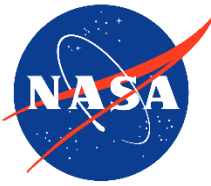


Volume rendering of  $Y_{H_2O}$



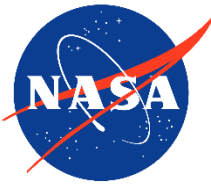
Shock with isosurfaces of  $Y_{H_2O} = 0.40$ , colored by vorticity magnitude  
(each Cartesian grid line represents 10 m)





# Impacts of Chemistry

- Dynamic similarity is maintained for various key parameters such as freestream Mach number, Reynolds number, nozzle exit-to-stagnation freestream pressure ratios, nozzle exit Mach number, and dynamic pressure
- Primary difference is incorporation of chemistry
- Flow structures for chemically reacting simulations are qualitatively similar to perfect gas air simulations
  - Throttling conditions investigated behave similarly
- Engine Thrust accounts for the majority of the axial force on the vehicle for both gas models
- Key differences include:
  - Specific heat ratio varies substantially in the nozzles and upstream of the vehicle due to strong temperature dependence of carbon dioxide and other species
  - Significant minor species concentrations including hydroxyl radical (~4%) upstream of the vehicle potentially impacting thermal design
  - Reacting gas simulations predict larger (40%+) aerodynamic axial forces compared to perfect gas air



# Summary and Future Work

- Full-scale, wall-resolved, chemically reacting computational fluid dynamics simulations have been completed for a conceptual human-scale Mars lander with retropropulsion at supersonic, transonic, and subsonic flight conditions
- All work was completed using the GPU-enabled version of the NASA FUN3D flow solver on Oak Ridge National Laboratory's Summit supercomputer
- Consistent with subscale experiments and past simulations, the aerodynamic contribution to total deceleration force during powered descent is small ( $< 6\%$  due to aerodynamics)
- Significant minor species concentrations are present upstream of the vehicle ( $Y_{OH} > 4\%$ ), and the specific heat ratio varies greatly both in the nozzles ( $\gamma$  varies from 1.19 to 1.26) and upstream of the vehicle
- Inclusion of chemistry is potentially required for vehicle thermal impacts
- Upcoming wind tunnel testing will provide subscale, inert gas validation data for several retropropulsion configurations with 4 and 8 nozzles
- Validation data for non-air inert and chemically-reacting simulant gases are still required

*This research used resources of the Oak Ridge Leadership Computing Facility at the Oak Ridge National Laboratory, which is supported by the Office of Science of the U.S. Department of Energy under Contract No. DE-AC05-00OR22725.*